

## COMPARISON OF EIGENFUNCTIONS COMPUTED FOR CYLINDRICAL CLOSED SHELLS BY AN ITERATIVE DECOUPLING PROCEDURE

*A general procedure for estimating eigenvalues is presented within the framework of a problem for an elastic thin closed shell implying its reduction to a differential equation of the eighth order. The idea implies decoupling of the problem into two simpler ones: a plane elasticity problem and a thin plate problem. Both problems are reduced to a biquadratic equation. By choosing one of these problems to be the main one, the corresponding functions for the other problem can be presented by a linear combination of functions obtained from the main problem. The derived eigenvalues are compared for the four dominant cylindrical-shell theories concerning the concentrated radial load. The results slightly differ only for small numbers of the circumferential mode expansion and agree with earlier results obtained through the use of different semi-analytical methods.*

**Key words:** cylindrical shell, decoupling procedure, eigenvalues, concentrated radial force, main homogeneous equation, auxiliary particular solution.

**Introduction.** A problem on the deformation of a cylindrical thin-walled shell under the action of a concentrated load can be considered as a coupling of two rather simple problems, i.e. a plane problem of elasticity (“membrane problem”) and a thin plate problem. Due to the actual curvature of the shell, the force from the “membrane problem” is projected onto the radial direction and the equilibrium equations involve the axial and circumferential displacements. When the curvature of the shell tends to zero, these two problems become quite independent and, thus, the general problem can be decoupled. The method, which we suggest in this paper, rests upon a similar logic. First, we consider both problems independent (decoupled). Then, we iteratively encounter the mutual effect of these problems on one another.

There exists a variety of the theories for the thin-walled cylindrical shells implying different physical and geometric assumptions. The most dominant approach is concerned with the decomposition of the involved functions into the Fourier series with respect to the circumferential coordinate and the determination of a coefficient for mode  $n$ . As a result, one can obtain an ordinary differential equation of the eighth order with respect to the axial coordinate. There are at least twelve different characteristic equations corresponding to different theories [10]. Despite the fact that some eigenfunctions were compared of specific modes, they have been computed through the use of a solution of a biquadratic equation failed to be given in a closed analytical form.

Nevertheless, these eigenfunctions can be found analytically for some simplified theories, e.g., the Donnell equation [23]. In [8], the simple expressions have been obtained for the eigenfunctions of the Flügge equation. Morley [13] derived another simplified equation providing an analytical solution. In [22], the differential equations of [15] were analyzed.

Summarizing the analysis of the eigenfunctions, we can emphasize the following features. First of all, it was shown in [8] that all eight eigenfunctions can be represented in the form

$$F_{1,2,3,4}(x) = e^{\mp a_n x} \begin{Bmatrix} \cos b_n x \\ \sin b_n x \end{Bmatrix}, \quad \Phi_{1,2,3,4}(x) = e^{\mp c_n x} \begin{Bmatrix} \cos d_n x \\ \sin d_n x \end{Bmatrix}. \quad (1)$$

Then for lower modes  $n \geq 2$ , the eigenfunctions can be split into two groups [5]: shortwave (first formula in (1)) and longwave (second formula in (1)) ones.

<sup>✉</sup> glibyudin@gmail.com

The longwave (“long”) solution can be regarded rather practical. It was derived by Vlasov [2] back in 1949 on the basis of the semi-membrane shell theory implying the circumferential and shear strains to be zeros. Vlasov’s theory has become quite popular due to its practical applications, e.g. for the evaluation of the end effects in the toroidal shells [1, 18] with concern to the concentrated force [14, 16], bending instability [11], buckling [24], analysis of vibration of conventional and short shells [20]. However, it contradicts the applicability of the shortwave (“short”) solution concerning, e.g., mitered bend under the inner pressure [6, 7].

According to Goldenveizer [3], the Vlasov’s hypothesis can be substituted with the following one: the solution is to vary in the circumferential direction faster than in the axial one, i.e.  $d^2\Omega/dx^2 \leq d^2\Omega/(Rd\varphi)^2$ , where  $\Omega$  is any parameter of the shell problem. This idea inspired us for our attempt. By analogy, we assumed that, if the “long” fourth-order solution satisfies the aforementioned requirement, then the supplemental “short” fourth-order solution must to exist and satisfy the requirement  $d^2\Omega/dx^2 \geq d^2\Omega/(Rd\varphi)^2$ .

Hence, both “long” and “short” solutions should be equally important. This idea was developed in our works [17, 21] and eventually polished in [19], where it was accounted that both solutions produce all eight components (shell parameters) of the complete solution.

This paper implies two goals. Firstly, we suggest the iterative decoupling procedure for finding the solutions to a characteristic equation. We start from a simple solution constructed for one of two uncoupled problems (membrane problem or plate one) and slowly refine them by taking into account the influence of another, “alien” uncoupled problem. It can be shown that the “long” solution corresponds to the membrane-generated problem, and the “short” solution to the plate-generated problem. Secondly, we examine four different formulations. For each of them, we compute the roots of characteristic equation and eigenfunctions, and validate their accuracy through the mutual comparison.

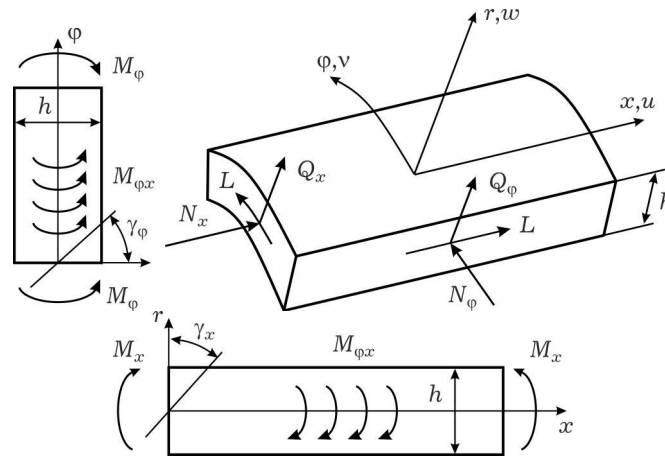


Fig. 1. Directions of geometrical and force parameters: plane  $(\varphi, r)$ , 3D view of the element, and plane  $(x, r)$ .

## 1. Formulation of the problem.

**1.1. General formulation of the problem for an infinite cylindrical shell.** Consider an infinite cylindrical shell of radius  $R$  related to the cylindrical system of coordinates  $(r, \varphi, x)$ . Consider  $u$ ,  $v$ , and  $w$  being the displacements.

cements,  $N_x$  and  $N_\varphi$  denoting the membrane forces,  $L$  standing for the shear force,  $Q_x$  and  $Q_\varphi$  being the transverse forces, and  $M_x$ ,  $M_\varphi$ , and  $M_{x\varphi}$  representing the bending moments (see Fig. 1). These functions are governed by the following equations

$$\frac{\partial N_x}{\partial x} + \frac{1}{R} \frac{\partial L}{\partial \varphi} = 0, \quad \frac{1}{R} \frac{\partial N_\varphi}{\partial \varphi} + \frac{\partial L}{\partial x} + \frac{Q_\varphi}{R} = 0, \quad \frac{\partial Q_x}{\partial x} + \frac{1}{R} \frac{Q_\varphi}{\partial \varphi} - \frac{N_\varphi}{R} = 0,$$

$$Q_x = \frac{M_x}{\partial x} + \frac{1}{R} \frac{\partial M_{x\varphi}}{\partial \varphi}, \quad Q_\varphi = \frac{1}{R} \frac{\partial M_\varphi}{\partial \varphi} + \frac{\partial M_{x\varphi}}{\partial x}$$

and related to the membrane and bending strains,  $\varepsilon_j, \varepsilon_{ij}, \gamma_j$  and  $\chi_j, \chi_{ij}$ , respectively,  $i, j = \{x, \varphi\}$ , via the following constitutive equations:

$$N_x = -(\varepsilon_x + \mu\varepsilon_\varphi)H, \quad N_\varphi = -(\varepsilon_\varphi + \mu\varepsilon_x)H, \quad L = -Gh\varepsilon_{x\varphi},$$

$$M_x = -(\chi_x + \mu\chi_\varphi)Hx, \quad M_\varphi = -(\chi_\varphi + \mu\chi_x)Hx, \quad M_{x\varphi} = \frac{\mu-1}{2}Hx\chi_{x\varphi},$$

where  $H = Eh/(1 - \mu^2)$ ,  $2G = E/(1 + \nu)$ ,  $x = h^2/12$ ,  $\mu$  is Poisson's ratio.

The strains are related to displacements via the geometric Cauchy equations

$$\varepsilon_x = \frac{\partial u}{\partial x}, \quad \varepsilon_\varphi = \frac{1}{R} \frac{\partial v}{\partial \varphi} + \frac{w}{R}, \quad \varepsilon_{x\varphi} = \frac{1}{R} \frac{\partial u}{\partial \varphi} + \frac{\partial v}{\partial x}. \quad (2)$$

Decompose the functions into the Fourier series with respect to the circumferential variable to obtain the following:

$$\{u(x, \varphi), w(x, \varphi)\} = \{u_n(x), w_n(x)\} \cos(n\varphi), \quad v(x, \varphi) = v_n(x) \sin(n\varphi),$$

$$\{N_j(x, \varphi), M_j(x, \varphi), Q_x(x, \varphi)\} = \{N_{j,n}(x), M_{j,n}(x), Q_{x,n}(x)\} \cos(n\varphi),$$

$$\{L(x, \varphi), Q_\varphi(x, \varphi), M_{x\varphi}(x, \varphi)\} = \{L_n(x), Q_{\varphi,n}(x), M_{x\varphi,n}(x)\} \sin(n\varphi),$$

where  $j = \{x, \varphi\}$ . In what follows, indices  $n$  will be omitted for the sake of brevity. The confusion between the Fourier coefficients and the original parameters will be avoided by indicating one or two arguments, respectively.

The encountering for the bending deformations depends on the specific formulation of the problem. In order to compare different cases, we consider the specific formulations below.

**1.2. Different approaches to the problem formulation.** According to the main hypotheses of shell theories, the total displacements  $\bar{u}$ ,  $\bar{v}$ , and  $\bar{w}$  can be given in the form, as follows:

$$\bar{u}(r, \varphi, x) = u(\varphi, x) + r\gamma_x(\varphi, x), \quad \bar{v}(r, \varphi, x) = v(\varphi, x) + r\gamma_\varphi(\varphi, x),$$

$$\bar{w}(r, \varphi, x) = w(\varphi, x). \quad (3)$$

Here,  $r$  is the radial coordinate that equals zero at the midsurface of the shell and takes negative and positive values in the direction of the inner and outer limiting surfaces, respectively.

Then, the membrane strains take the form [12]:

$$\bar{\varepsilon}_r = \frac{\partial \bar{w}}{\partial r}, \quad \bar{\varepsilon}_\varphi = \frac{1}{R+r} \frac{\partial \bar{v}}{\partial \varphi} + \frac{\bar{w}}{R+r}, \quad \bar{\varepsilon}_x = \frac{\partial \bar{u}}{\partial x}, \quad \bar{\varepsilon}_{xr} = \frac{\partial \bar{w}}{\partial x} + \frac{\partial \bar{u}}{\partial r},$$

$$\bar{\varepsilon}_{r\varphi} = \frac{1}{R+r} \frac{\partial \bar{w}}{\partial \varphi} + \frac{\partial \bar{v}}{\partial r} - \frac{\bar{v}}{R+r}, \quad \bar{\varepsilon}_{x\varphi} = \frac{\partial \bar{v}}{\partial x} + \frac{1}{R+r} \frac{\partial \bar{u}}{\partial \varphi}. \quad (4)$$

When engaging the theory of thin shells, the transverse forces  $Q_\varphi$  and  $Q_x$ , and, hence, the strains induced by these forces are negligible. Within the context of formulas (4), this implies the following:

$$\frac{1}{R+r} \frac{\partial \bar{w}}{\partial \varphi} + \frac{\partial \bar{v}}{\partial r} - \frac{\bar{v}}{R+r} = 0, \quad \frac{\partial \bar{w}}{\partial x} + \frac{\partial \bar{u}}{\partial r} = 0. \quad (5)$$

Making use of (3) for the first formula in (5) yields

$$\frac{1}{R+r} \frac{\partial w}{\partial \varphi} + \gamma_\varphi(\varphi, x) - \frac{v(\varphi, x)}{R+r} - \frac{r\gamma_\varphi(\varphi, x)}{R+r} = 0.$$

Restricting ourselves with the linear terms of the Taylor series for  $\gamma_\varphi$  and implying  $1/(R+r) \approx (1-r/R)/R$ , we arrive at

$$\gamma_\varphi(\varphi, x) = -\frac{1}{R} \frac{\partial w}{\partial \varphi} + \frac{v(\varphi, x)}{R}.$$

Now we use (3) within the context of the second formula in (5) to obtain

$$\gamma_x(\varphi, x) = -\frac{\partial w(\varphi, x)}{\partial x}.$$

In view of the fact that within the framework of the adopted shell theory  $\bar{\varepsilon}_r = 0$ , we address the strains  $\bar{\varepsilon}_\varphi$ ,  $\bar{\varepsilon}_x$ , and  $\bar{\varepsilon}_{x\varphi}$ , which in view of the corresponding formulas in (3) and (4) yield the linear dependencies

$$\bar{\varepsilon}_j = \varepsilon_j + r\chi_j, \quad \bar{\varepsilon}_{x\varphi} = \varepsilon_{x\varphi} + r\chi_{x\varphi}, \quad j = \{x, \varphi\}. \quad (6)$$

By decomposing these strains into the Taylor series with respect to the ratio  $r/R$  and encountering only the linear terms, we can compare the obtained formulas with (5) which yields formulas (2) along with the expressions

$$\begin{aligned} \chi_\varphi &= -\frac{1}{R^2} \frac{\partial^2 w}{\partial \varphi^2} - \frac{w}{R^2}, & \chi_x &= -\frac{\partial^2 w}{\partial x^2}, \\ \chi_{x\varphi} &= -\frac{2}{R} \frac{\partial^2 w}{\partial \varphi \partial x} + \frac{1}{R} \frac{\partial v}{\partial x} - \frac{1}{R^2} \frac{\partial u}{\partial \varphi}. \end{aligned} \quad (7)$$

As indicated above, the derived formulas (7) are based on the linear approximation for the term  $1/(r+R)$ . This can be done based on other assumptions. If, for instance,  $1/(r+R) \approx 1/R$ , i.e.,  $(1+r/R) \approx 1$ , then using the above approach, we can derive

$$\begin{aligned} \chi_\varphi &= -\frac{1}{R^2} \frac{\partial^2 w}{\partial \varphi^2} + \frac{1}{R^2} \frac{\partial v}{\partial \varphi}, & \chi_x &= -\frac{\partial^2 w}{\partial x^2}, \\ \chi_{x\varphi} &= -\frac{2}{R} \frac{\partial^2 w}{\partial \varphi \partial x} + \frac{1}{R} \frac{\partial v}{\partial x}. \end{aligned} \quad (8)$$

Using approach [19] which implies the radial strain to be the linear part of the membrane strains, we arrive at

$$\chi_\varphi = -\frac{1}{R^2} \frac{\partial^2 w}{\partial \varphi^2} - \frac{w}{R^2}, \quad \chi_x = -\frac{\partial^2 w}{\partial x^2}, \quad \chi_{x\varphi} = -\frac{2}{R} \frac{\partial^2 w}{\partial \varphi \partial x}. \quad (9)$$

Finally, making use of Donnell – Mushtari – Vlasov theory, we can obtain

$$\chi_\varphi = -\frac{1}{R^2} \frac{\partial^2 w}{\partial \varphi^2}, \quad \chi_x = -\frac{\partial^2 w}{\partial x^2}, \quad \chi_{x\varphi} = -\frac{2}{R} \frac{\partial^2 w}{\partial \varphi \partial x}. \quad (10)$$

**2. Problem decomposition.** The suggested approach implies the decomposition of the formulated general problem into two coupled problems: a membrane problem and a plate problem. The equilibrium equations in the axial and circumferential directions are governed by the membrane problem, while the ones in the radial direction are concerned with the plate problem. Due to the non-zero curvature, the radial force can be projected onto the circumferential direction.

Within the framework of our approach, one of these coupled problems is regarded as a main one, while the other problem is the auxiliary one. The objective of the main problem is to generate the eigenfunctions using the structure of formulae (1) allowing for the homogenization of the governing equations. The auxiliary problem implies correction of the eigenfunctions.

Let us demonstrate the suggested algorithm for the case presented by formulae (7).

Consider the equilibrium equations in projections onto the radial, circumferential, and axial directions in the following form:

$$\begin{aligned} \frac{d^2u}{dx^2} + \alpha_{v,1} \frac{dv}{dx} + \alpha_{u,0}u &= \text{RS1}, \\ \beta_{v,2} \frac{d^2v}{dx^2} + \beta_{u,1} \frac{du}{dx} + \beta_{v,0}v &= \text{RS2}, \\ \gamma_{w,4} \frac{d^4w}{dx^4} + \gamma_{w,2} \frac{d^2w}{dx^2} + \gamma_{w,0}w &= \text{RS3}. \end{aligned} \quad (11)$$

Here,

$$\begin{aligned} \alpha_{v,1} &= \frac{n(1+\mu)}{2R}, \quad \alpha_{u,0} = -\frac{n^2(1-\mu)}{2R^2}, \quad \text{RS1} = -\frac{\mu}{R} \frac{dw}{dx}, \\ \beta_{v,2} &= -\frac{1-\mu}{2} \left(1 + \frac{x}{R^2}\right), \quad \beta_{u,1} = \frac{n(1+\mu)}{2R}, \quad \beta_{v,0} = \left(1 + \frac{x}{R^2}\right) \frac{n^2}{R^2}, \\ \text{RS2} &= \frac{n}{R^2} \left( x \frac{d^2w}{dx^2} - \left(1 + x \frac{n^2}{R^2}\right) w \right), \end{aligned} \quad (12)$$

$$\begin{aligned} \gamma_{w,4} &= x, \quad \gamma_{w,2} = -2x \frac{n^2}{R^2}, \quad \gamma_{w,0} = \frac{1}{R^2} \left(1 + x \frac{n^4}{R^2}\right), \\ \text{RS3} &= \frac{n}{R^2} \left( x \frac{d^2v}{dx^2} - \left(1 + x \frac{n^2}{R^2}\right) v \right) - \frac{\mu}{R} \frac{du}{dx}. \end{aligned} \quad (13)$$

The first and second equations in (11) govern the membrane problem, while the third one complies with the plate problem.

**Step 1 (solving the main problem).** Assume existence of  $c_u, c_v, d_u, d_v \in \mathbb{R}$  allowing for the following representation:

$$\text{RS1} = c_u u + c_v \frac{dv}{dx}, \quad \text{RS2} = d_u \frac{du}{dx} + d_v v.$$

The first iteration implies  $c_u = c_v = d_u = d_v = 0$ . This means that the main and auxiliary problems are decoupled. For the following steps, we have

$$\begin{aligned} \frac{d^2u}{dx^2} + (\alpha_{v,1} - c_v) \frac{dv}{dx} + (\alpha_{u,0} - c_u)u &= 0, \\ \beta_{v,2} \frac{d^2v}{dx^2} + (\beta_{u,1} - d_u) \frac{du}{dx} + (\beta_{v,0} - d_v)v &= 0. \end{aligned} \quad (14)$$

Equations (14) can be reduced to the following fourth-order equation:

$$\frac{d^4 u}{dx^4} + \eta_2 \frac{d^2 u}{dx^2} + \eta_4 u = 0.$$

where  $\eta_2 = (\alpha_{u,0} - c_u) + \frac{\beta_{v,0} - d_v}{\beta_{v,2}} - (\alpha_{v,1} - c_v) \frac{\beta_{u,1} - d_u}{\beta_{v,2}}$ ,  $\eta_4 = (\alpha_{u,0} - c_u) \frac{\beta_{v,0} - d_u}{\beta_{v,2}}$ .

This equation generates the following eigenvalues:

$$\lambda_m = \pm \sqrt{\frac{-\eta_2 \pm \sqrt{\eta_2^2 - 4\eta_4}}{2}} = \pm c \pm id,$$

$$c = |\operatorname{Re}(\lambda_m)|, \quad d = |\operatorname{Im}(\lambda_m)|.$$

The corresponding eigenfunctions those are bounded at the infinitely distant points  $|x| \rightarrow \infty$ , take the form:

$$\Phi_1(x) = \exp(-cx) \cos(dx), \quad \Phi_2(x) = \exp(-cx) \sin(dx). \quad (15)$$

If  $d = 0$ , which is the case, e.g., for the first iteration, then the form of the eigenfunctions will naturally be different. In this case, the eigenvalues are real and equal  $\pm n / R$ . For such cases, however, we introduce minor complex disturbance  $d = 0.001n / R$  in order to preserve the form (15).

Note that functions (15) have the following features:

$$\begin{pmatrix} \dot{\Phi}_1 \\ \dot{\Phi}_2 \end{pmatrix} = \mathbf{\Pi} \begin{pmatrix} \Phi_1 \\ \Phi_2 \end{pmatrix}, \quad \int \begin{pmatrix} \Phi_1 \\ \Phi_2 \end{pmatrix} dx = \mathbf{\Pi}^{-1} \begin{pmatrix} \Phi_1 \\ \Phi_2 \end{pmatrix}, \quad \mathbf{\Pi} = \begin{pmatrix} -c_n & -d_n \\ d_n & -c_n \end{pmatrix}, \quad (16)$$

where the dot indicates the derivative by  $x$ .

Within the context of (15), we can express the displacements in the form:

$$\begin{pmatrix} u(x) \\ v(x) \end{pmatrix} = \begin{pmatrix} 1 & 0 \\ A_{v,1} & A_{v,2} \end{pmatrix} \begin{pmatrix} \Phi_1(x) \\ \Phi_2(x) \end{pmatrix}, \quad (17)$$

where  $A_{v,1}$  and  $A_{v,2}$  are to be found from the first equation of (14), which in view of (17) yields

$$(A_{v,1} \ A_{v,2}) \begin{pmatrix} \dot{\Phi}_1(x) \\ \dot{\Phi}_2(x) \end{pmatrix} = (1 \ 0) \left( \frac{1}{c_v - \alpha_{v,1}} \begin{pmatrix} \ddot{\Phi}_1(x) \\ \ddot{\Phi}_2(x) \end{pmatrix} - \frac{\alpha_{u,0} - c_u}{\alpha_{v,1} - c_v} \begin{pmatrix} \Phi_1(x) \\ \Phi_2(x) \end{pmatrix} \right).$$

This formula along with the properties (16) allow for deriving the following:

$$(A_{v,1} \ A_{v,2}) \begin{pmatrix} \Phi_1(x) \\ \Phi_2(x) \end{pmatrix} = (1 \ 0) \left( \frac{1}{c_v - \alpha_{v,1}} \mathbf{\Pi} - \frac{\alpha_{u,0} - c_u}{\alpha_{v,1} - c_v} \mathbf{\Pi}^{-1} \right) \begin{pmatrix} \Phi_1(x) \\ \Phi_2(x) \end{pmatrix}.$$

Solving the latter equation with respect to  $A_{v,1}$  and  $A_{v,2}$  concludes the step 1.

**Step 2 (auxiliary problem).** Now we intend to construct function

$$w(x) = A_{w,1}(x)\Phi_1(x) + A_{w,2}(x)\Phi_2(x), \quad (18)$$

by putting functions (17) into the third equation of (11), which yields:

$$\begin{aligned} (A_{w,1} \ A_{w,2}) \left( \gamma_{w,4} \mathbf{\Pi}^4 + \gamma_{w,2} \mathbf{\Pi}^2 + \gamma_{w,0} \mathbf{\Pi}^0 \right) \begin{pmatrix} \Phi_1 \\ \Phi_2 \end{pmatrix} = \\ = \left( (A_{v,1} \ A_{v,2}) \frac{\mathfrak{x}n}{R^2} \mathbf{\Pi}^2 - (1 \ 0) \frac{\mu}{R} \mathbf{\Pi} + \right. \\ \left. - (A_{v,1} \ A_{v,2}) \left( \frac{\mathfrak{x}n^3}{R^4} - \frac{n}{R^2} \right) \mathbf{\Pi}^0 \right) \begin{pmatrix} \Phi_1 \\ \Phi_2 \end{pmatrix}, \end{aligned}$$

where  $\Pi^0$  is the unit matrix. Solving this equation allows for the determination of  $A_{w,1}$  and  $A_{w,2}$ , which finalizes the determination of the function (18).

In order to complete the cycle and begin the next iteration, we shall determine the values for  $c_j$  and  $d_j$ ,  $j = \{u, w\}$ , which allow for the satisfaction of (12) and (13). After these values are found, we switch back to solving the main problem (step 1) again implying the results of the supplementary problem to be the main ones.

### 3. Convergence.

It should be noted that for many iterative processes, the suggested separation algorithm encounter the convergence problems due to the fact that for greater values of  $n$  (starting, e.g., from  $n = 9$  as it might be seen from Fig. 2), the eigenvalues exhibit the oscillating behavior, and, in the final count, the algorithm appears to be divergent.

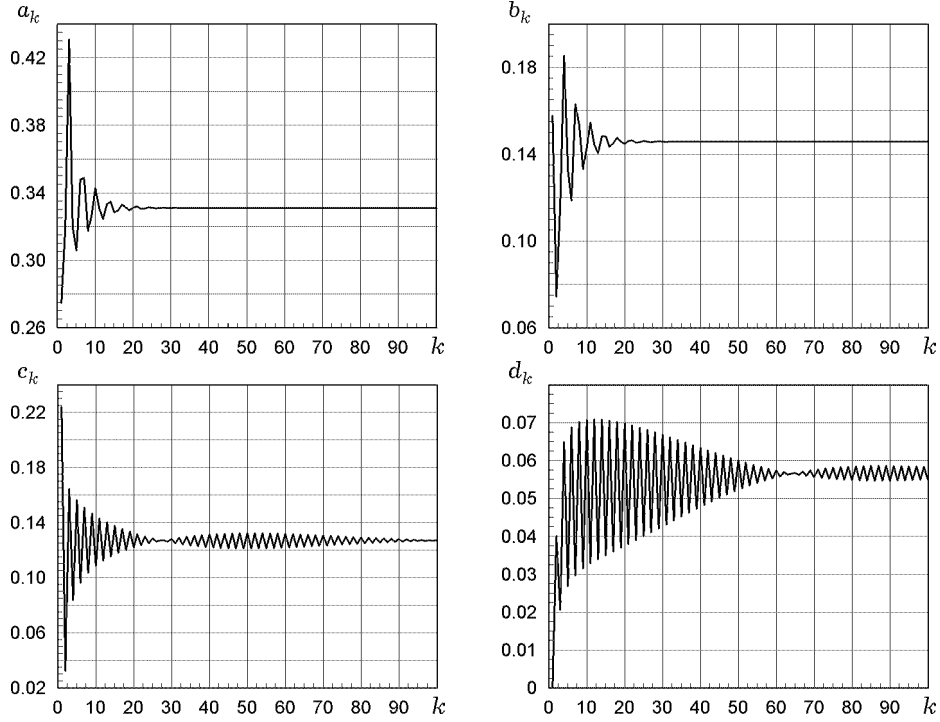


Fig. 2. Oscillations of the eigenvalues at  $R / h = 40$  and  $n = 9$ .

This can be fixed by slowing the variation of the coefficients in the following manner. Assume the coefficients  $c_j^{i-1}$  and  $d_j^{i-1}$ ,  $j = \{u, v\}$ , were found on the  $(i - 1)$ th iteration. The values of the coefficients on the current operation are being changed to the values  $c_j^i - c_j^{i-1}$  and  $d_j^i - d_j^{i-1}$ . In order to prevent the divergence, we minimize the absolute values of these differences by introducing the delay coefficient  $0 \leq \rho \leq 1$  so that

$$c_j^{i,\text{adjusted}} = c_j^{i-1,\text{adjusted}} + \rho(c_j^i - c_j^{i-1,\text{adjusted}}),$$

with an analogous formula for coefficient  $d_j^{i,\text{adjusted}}$ . This procedure can be applied, if necessary, to all values determined within the algorithm routine.

**4. Results and discussion.** We used the four approaches above, implying representations (7) – (10), in order to compute the eigenfunctions

$$\Phi_1(x) = e^{-cx} \cos(dx), \quad \Phi_2(x) = e^{-cx} \sin(dx),$$

$$F_1(x) = e^{-ax} \cos(bx), \quad F_2(x) = e^{-ax} \sin(bx).$$

Tables 1–3 present computed coefficients  $c$ ,  $d$ ,  $a$ ,  $b$  for each approach. All the results will be compared with the results obtained for the case of (8) by evaluating the relative difference  $\theta$  [%] at different  $n$  and  $R/h$ .

Table 1. Coefficients  $c$ ,  $d$ ,  $a$ ,  $b$  computed through the four approaches at  $R/h = 20$ .

$R/h = 20$		Eqs. (7)		Eqs. (8)		Eqs. (9)		Eqs. (10)	
		value	$\theta, \%$	value	$\theta, \%$	value	$\theta, \%$	value	$\theta, \%$
$n = 2$	$c$	0.015738	0.16	0.015713	–	0.015796	0.53	0.016969	7.99
	$d$	0.014221	0.22	0.014253	–	0.014153	0.7	0.015202	6.66
	$a$	0.305475	0.11	0.305125	–	0.305208	0.03	0.305606	0.16
	$b$	0.270854	0.11	0.271152	–	0.271250	0.04	0.271020	0.05
$n = 5$	$c$	0.115883	0.01	0.115866	–	0.116051	0.16	0.117138	1.1
	$d$	0.064541	0.25	0.064702	–	0.064120	0.9	0.064737	0.05
	$a$	0.405488	0.09	0.405140	–	0.405332	0.05	0.405673	0.13
	$b$	0.220668	0.08	0.220842	–	0.221417	0.26	0.221587	0.34
$n = 10$	$c$	0.356058	0.02	0.356124	–	0.356244	0.03	0.357019	0.25
	$d$	0.103821	0.26	0.104087	–	0.102762	1.27	0.103189	0.86
	$a$	0.645651	0.04	0.645365	–	0.645512	0.02	0.645544	0.03
	$b$	0.181400	0.05	0.181492	–	0.182788	0.71	0.183143	0.91
$n = 20$	$c$	0.854961	0.02	0.855112	–	0.855163	0.01	0.855737	0.07
	$d$	0.126859	0.32	0.127270	–	0.124568	2.12	0.124964	1.81
	$a$	1.144569	0.03	1.144281	–	1.144443	0.01	1.144275	0
	$b$	0.158347	0.02	0.158381	–	0.160970	1.63	0.161355	1.88

Table 2 Coefficients  $c$ ,  $d$ ,  $a$ ,  $b$  computed through the four approaches at  $R/h = 30$ .

$R/h = 30$		Eqs. (7)		Eqs. (8)		Eqs. (9)		Eqs. (10)	
		value	$\theta, \%$	value	$\theta, \%$	value	$\theta, \%$	value	$\theta, \%$
$n = 2$	$c$	0.008457	0.12	0.008447	–	0.008479	0.38	0.009110	7.85
	$d$	0.007902	0.14	0.007913	–	0.007878	0.44	0.008463	6.95
	$a$	0.244401	0.08	0.244214	–	0.244246	0.01	0.244451	0.1
	$b$	0.225504	0.07	0.225672	–	0.225707	0.02	0.225563	0.05
$n = 5$	$c$	0.064114	0.03	0.064097	–	0.064195	0.15	0.064823	1.13
	$d$	0.041600	0.16	0.041667	–	0.041438	0.55	0.041828	0.39
	$a$	0.299985	0.07	0.299790	–	0.299889	0.03	0.300108	0.11
	$b$	0.191879	0.06	0.191992	–	0.192220	0.12	0.192254	0.14
$n = 10$	$c$	0.217369	0.01	0.217392	–	0.217467	0.03	0.217936	0.25
	$d$	0.076762	0.17	0.076889	–	0.076310	0.75	0.076555	0.43
	$a$	0.453232	0.04	0.453072	–	0.453153	0.02	0.453215	0.03
	$b$	0.156725	0.04	0.156784	–	0.157356	0.36	0.157533	0.48
$n = 20$	$c$	0.548767	0.01	0.548831	–	0.548869	0.01	0.549208	0.07
	$d$	0.098274	0.19	0.098460	–	0.097271	1.21	0.097487	0.99
	$a$	0.784633	0.02	0.784492	–	0.784557	0.01	0.784489	0
	$b$	0.135211	0.01	0.135231	–	0.136393	0.86	0.136599	1.01



Table 3. Coefficients  $c$ ,  $d$ ,  $a$ ,  $b$  computed through the four approaches at  $R/h = 40$ .

$R/h = 40$		Eqs. (7)		Eqs. (8)		Eqs. (9)		Eqs. (10)	
		value	$\theta, \%$	value	$\theta, \%$	value	$\theta, \%$	value	$\theta, \%$
$n = 2$	$c$	0.005454	0.09	0.005449	–	0.005465	0.29	0.005872	7.76
	$d$	0.005183	0.12	0.005189	–	0.005171	0.35	0.005556	7.07
	$a$	0.209515	0.06	0.209396	–	0.209411	0.01	0.209540	0.07
	$b$	0.197230	0.06	0.197341	–	0.197357	0.01	0.197258	0.04
$n = 5$	$c$	0.041535	0.03	0.041523	–	0.041582	0.14	0.041999	1.15
	$d$	0.029553	0.11	0.029587	–	0.029472	0.39	0.029753	0.56
	$a$	0.245550	0.05	0.245422	–	0.245481	0.02	0.245631	0.09
	$b$	0.172908	0.05	0.172990	–	0.173104	0.07	0.173098	0.06
$n = 10$	$c$	0.150899	0.01	0.150908	–	0.150961	0.04	0.151290	0.25
	$d$	0.061006	0.12	0.061081	–	0.060761	0.52	0.060930	0.25
	$a$	0.354908	0.03	0.354799	–	0.354855	0.02	0.354918	0.03
	$b$	0.141460	0.03	0.141503	–	0.141820	0.22	0.141925	0.3
$n = 20$	$c$	0.398210	0.01	0.398245	–	0.398274	0.01	0.398508	0.07
	$d$	0.081816	0.13	0.081926	–	0.081260	0.81	0.081401	0.64
	$a$	0.602219	0.01	0.602129	–	0.602168	0.01	0.602136	0
	$b$	0.120650	0.01	0.120666	–	0.121322	0.54	0.121453	0.65

Evidently, the results for all the approaches resemble for  $n \geq 5$  as their difference is less than  $(1 \div 2)\%$ . For the smaller values of  $n$ , however, the fourth case (the Donnell – Mushtari – Vlasov approximate theory) deviates over 7%. This confirms the results of [4] indicating this theory to be more or less exact for the modes with greater values of  $n$ , i.e., when  $1/n^2 \leq 1$ .

Consider the action of a concentrated force implying the following boundary conditions:

$$u|_{x=0} = 0, \quad \gamma_x|_{x=0} = 0, \quad L|_{x=0} = 0, \quad Q_x|_{x=0} = P/2,$$

$$P(x, \varphi) = 2\delta(x) \cos(nx).$$

Here,  $\delta(x)$  is the Dirac function.

Table 4. Normalized values of radial displacement  $\tilde{w}$  and bending moment  $\tilde{M}_x$  at  $x = 0$  and  $R/h = 20$ .

$R/h = 20$		Eqs. (7)		Eqs. (8)		Eqs. (9)		Eqs. (10)	
		value	$\theta, \%$	value	$\theta, \%$	value	$\theta, \%$	value	$\theta, \%$
$n = 2$	$\tilde{w}(0)$	1.864815	0.17	1.868084	–	1.857412	0.57	1.524150	18.41
	$\tilde{M}_x(0)$	1.478418	0.03	1.477967	–	1.474964	0.2	1.502798	1.68
$n = 5$	$\tilde{w}(0)$	0.194101	0.12	0.194338	–	0.193662	0.35	0.188648	2.93
	$\tilde{M}_x(0)$	1.324107	0.05	1.324832	–	1.321872	0.22	1.321451	0.26
$n = 10$	$\tilde{w}(0)$	0.026330	0.03	0.026338	–	0.026308	0.11	0.026134	0.77
	$\tilde{M}_x(0)$	0.742840	0.02	0.743003	–	0.742412	0.08	0.742088	0.12
$n = 20$	$\tilde{w}(0)$	0.003286	0	0.003286	–	0.003285	0.03	0.003280	0.18
	$\tilde{M}_x(0)$	0.373819	0.01	0.373839	–	0.373749	0.02	0.373705	0.04
$n = 40$	$\tilde{w}(0)$	0.000410	0	0.000410	–	0.000410	0	0.000410	0
	$\tilde{M}_x(0)$	0.186877	0	0.186880	–	0.186861	0.01	0.186856	0.01

Consider the computation of the dimensionless displacement and bending moment:

$$\tilde{w} = w / C_w, \quad \tilde{M}_x = M_x / C_M,$$

$$C_w = \frac{(1 - \mu^2)^{3/4}}{E} \left( \frac{R}{h} \right)^{5/2}, \quad C_M = \frac{-\sqrt{Rh}}{2\sqrt[4]{3(1 - \mu^2)}}.$$

Table 5. Normalized values of radial displacement  $\tilde{w}$  and bending moment  $\tilde{M}_x$  at  $x = 0$  and  $R/h = 30$ .

$R/h = 30$		Eqs. (7)		Eqs. (8)		Eqs. (9)		Eqs. (10)	
		value	$\theta, \%$	value	$\theta, \%$	value	$\theta, \%$	value	$\theta, \%$
$n = 2$	$\tilde{w}(0)$	1.834894	0.12	1.837105	–	1.829958	0.39	1.494346	18.66
	$\tilde{M}_x(0)$	1.441217	0.03	1.440751	–	1.438956	0.12	1.466755	1.8
$n = 5$	$\tilde{w}(0)$	0.211476	0.1	0.211686	–	0.211099	0.28	0.205695	2.83
	$\tilde{M}_x(0)$	1.441131	0.03	1.441576	–	1.439222	0.16	1.440111	0.1
$n = 10$	$\tilde{w}(0)$	0.031850	0.04	0.031862	–	0.031827	0.11	0.031618	0.77
	$\tilde{M}_x(0)$	0.898627	0.02	0.898816	–	0.898149	0.07	0.897792	0.11
$n = 20$	$\tilde{w}(0)$	0.004021	0.02	0.004022	–	0.004020	0.05	0.004014	0.2
	$\tilde{M}_x(0)$	0.457453	0.01	0.457478	–	0.457381	0.02	0.457328	0.03
$n = 40$	$\tilde{w}(0)$	0.000502	0	0.000502	–	0.000502	0	0.000502	0
	$\tilde{M}_x(0)$	0.228859	0	0.228862	–	0.228846	0.01	0.228839	0.01

Table 6. Normalized values of radial displacement  $\tilde{w}$  and bending moment  $\tilde{M}_x$  at  $x = 0$  and  $R/h = 40$ .

$R/h = 40$		Eqs. (7)		Eqs. (8)		Eqs. (9)		Eqs. (10)	
		value	$\theta, \%$	value	$\theta, \%$	value	$\theta, \%$	value	$\theta, \%$
$n = 2$	$\tilde{w}(0)$	1.817302	0.09	1.818972	–	1.813599	0.3	1.476783	18.81
	$\tilde{M}_x(0)$	1.419971	0.03	1.419561	–	1.418289	0.09	1.445827	1.85
$n = 5$	$\tilde{w}(0)$	0.217785	0.08	0.217957	–	0.217468	0.22	0.211906	2.78
	$\tilde{M}_x(0)$	1.482535	0.01	1.482756	–	1.480961	0.12	1.482836	0.01
$n = 10$	$\tilde{w}(0)$	0.036174	0.04	0.036188	–	0.036151	0.1	0.035913	0.76
	$\tilde{M}_x(0)$	1.020621	0.02	1.020822	–	1.020106	0.07	1.019753	0.1
$n = 20$	$\tilde{w}(0)$	0.004638	0	0.004638	–	0.004637	0.02	0.004629	0.19
	$\tilde{M}_x(0)$	0.527626	0.01	0.527656	–	0.527550	0.02	0.527489	0.03
$n = 40$	$\tilde{w}(0)$	0.000580	0	0.000580	–	0.000580	0	0.000579	0.17
	$\tilde{M}_x(0)$	0.264242	0	0.264246	–	0.264230	0.01	0.264222	0.01

The results shown in Tables 4–6 agree well with the previous ones: the consideration of equations (7) and (9) exhibits high accuracy with difference no greater than 0.6%, while the implementation of (10) provides good accuracy only for greater values of  $n$ . At  $n = 2$ , the error for the latter case exceeds 19%. For the bending moments, this error is smaller. This can be explained by the fact that the Donnell – Mushtari – Vlasov theory neglects  $w$  in the expression for  $\chi_\varphi$ , but keeps the term with its second derivative. Therefore, the difference for the bending moment  $\tilde{M}_x$ , which also contains the second derivative of  $\tilde{w}$ , is smaller, while the results for  $\tilde{w}$  itself are not as satisfactory.

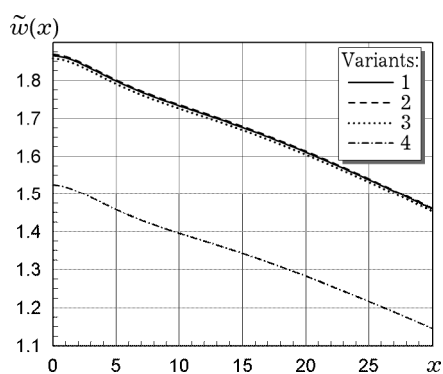


Fig. 3. The normalized radial displacement  $\tilde{w}(x)$  at  $n = 2$ ,  $R/h = 20$ .

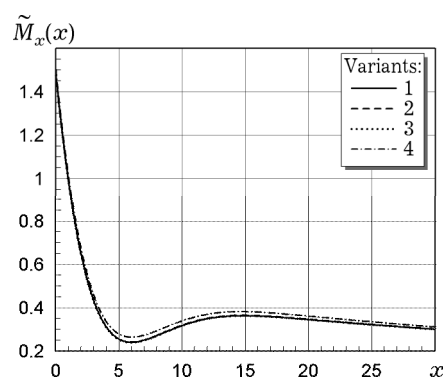


Fig. 4. The normalized bending moment  $\tilde{M}_x(x)$  at  $n = 2$ ,  $R/h = 20$ .

The foregoing conclusion is confirmed in Fig. 3 and Fig. 4, which demonstrate the dimensionless displacement and bending moment computed for four different variants presented by (7)–(10) at  $n = 2$  and  $R/h = 20$ .

**Conclusions.** Herein, the problem for a cylindrical infinite shell under the concentrated radial load is considered as a coupling of two problems, i.e. the “membrane” and “plate” one. An iterative decoupling method is introduced for solving these coupled problems. One of the problems is considered as a main one and is used to compute eigenfunctions. The other problem is considered as an auxiliary one and is used to refine obtained eigenfunctions. This procedure can be applied not only to the cylindrical shell, but, in general, to any coupled problem allowing to express the “alien” terms of the main equation via its “native” terms.

Another finding of this work is the comparison of different approaches for the formulation of a problem for cylindrical shells. We examined four different variants of equations derivation, including the well-known Donnell – Mushtari – Vlasov approximate theory. For each of these approaches, the decoupling procedure was applied to calculate eigenfunctions. Starting from  $n = 5$ , all these four theories produce similar results, their relative difference rarely exceeds 2% for real and imaginary parts of eigenvalues. However, for small values of  $n$  the Donnell – Mushtari – Vlasov theory is insufficient for producing accurate results, with relative error for dimensionless radial displacement being almost equal to 20%. Meanwhile, the other three approaches still returned values close to each other, which allows to use any of these theories in practical cases.

1. Аксельрад Э. Л. Гибкие оболочки. – Москва: Наука, 1976. – 376 с.
2. Власов В. З. Общая теория оболочек и ее приложения в технике. – Москва: Гостехиздат, 1949. – 784 с.
3. Гольденвейзер А. Л. Теория упругих тонких оболочек. – Москва: ГТТИ, 1953. – 544 с.
4. Amabili M. Nonlinear theories of elasticity of plates and shells // In: Nonlinear vibrations and stability of shells and plates. – Cambridge: Cambridge University Press, 2008. – 374 p. – (Chap. 1. – P. 6–51).  
– <https://doi.org/10.1017/CBO9780511619694.003>.
5. Calladine C. R. Theory of shell structures. – Cambridge: Cambridge University Press, 1983. – 763 p. – <https://doi.org/10.1017/CBO9780511624278>.
6. Feier I. I., Leis B. N., Zhu X. K., Stonesifer R. B., Stavarakas J. S., D’Eletto D. Experimental strain measurements on large diameter mitred pipe joints // Proc. of the 8th International Pipeline Conference (September 27 – October 1, 2010, Calgary, Canada). – Vol. 1. – Paper No. IPC2010-31583. – P. 881–891.  
– <https://doi.org/10.1115/IPC2010-31583>.

7. Green A. E., Emmerson W. C. Stresses in a pipe with a discontinuous bend // *J. Mech. Phys. Solids*. – 1961. – **9**, No. 2. – P. 91–104.  
– [https://doi.org/10.1016/0022-5096\(61\)90027-8](https://doi.org/10.1016/0022-5096(61)90027-8).
8. Holand I. Characteristic equations in the theory of circular cylindrical shells // *Aeronaut. Quart.* – 1962. – **13**, No. 1. – P. 88–91.  
– <https://doi.org/10.1017/S0001925900002262>.
9. Holand I. Design of circular cylindrical shells. – Oslo: Oslo University Press, 1957. – 253 p.
10. Houghton D. S., Johns D. J. A comparison of the characteristic equations in the theory of circular cylindrical shells // *Aeronaut. Quart.* – 1961. – **12**, No. 3. – P. 228–236. – <https://doi.org/10.1017/S0001925900002080>.
11. Karamanos S. A. Bending instabilities of elastic tubes // *Int. J. Solids Struct.* – 2002. – **39**, No. 8. – P. 2059–2085. – [https://doi.org/10.1016/S0020-7683\(02\)00085-9](https://doi.org/10.1016/S0020-7683(02)00085-9).
12. Love A. E. H. A treatise on the mathematical theory of elasticity. – New York: Dover, 1944. – 643 p.
13. Morley L. S. D. An improvement on Donnell's approximation for thin-walled circular cylinders. – *The Quart. J. Mech. Appl. Math.* – 1959. – **12**, No. 1. – P. 89–99. – <https://doi.org/10.1093/qjmam/12.1.89>.
14. Nerubailo B. V. Radial displacement of a long cylindrical shell subjected to radial concentrated forces // *Sov. Appl. Mech.* – 1974. – **10**, No. 10. – P. 1128–1131.  
– <https://doi.org/10.1007/BF00882358>.
15. Niordson F. I. Shell theory. – New York: Elsevier Science, 1985. – 408 p. – North-Holland series in applied mathematics and mechanics. – Vol. 29.
16. Ol'shanskii V. P. Maximal deflection of cylindrical shells under a concentrated force // *Strength Mater.* – 1990. – **22**, No. 10. – P. 1523–1526.  
– <https://doi.org/10.1007/BF00767243>.
17. Oryniak A., Orynyak I. Application of short and long (enhanced Vlasov's) solutions for cylindrical shell on example of concentrated radial force // *ASME J. Pressure Vessel Technol.* – 2021. – **143**, No. 1. – Art. 014501. – 11 p.  
– <https://doi.org/10.1115/1.4047828>.
18. Orynyak I. V., Radchenko S. A. Analytical and numerical solution for a elastic pipe bend at in-plane bending with consideration for the end effect // *Int. J. Solids Struct.* – 2007. – **44**, No. 5. – P. 1488–1510.  
– <https://doi.org/10.1016/j.ijsolstr.2006.06.025>.
19. Orynyak I., Bai Y. Coupled approximate long and short solutions versus exact Navier and Galerkin ones for cylindrical shell under radial load // *Thin-Walled Structures*. – 2022. – **170**. – Art. 108536.  
– <https://doi.org/10.1016/j.tws.2021.108536>.
20. Orynyak I., Dubyk Y. Approximate formulas for cylindrical shell free vibration based on Vlasov's and enhanced Vlasov's semi-momentless theory // *Proc. of ASME 2018 Pressure Vessels and Piping Conference (July 15–20, 2018, Prague, Czech Republic)*. – Vol. 8. – 2018. – Paper No. PVP2018-84932, V008T08A050. – 10 p. – <https://doi.org/10.1115/PVP2018-84932>.
21. Orynyak I., Oryniak A. Efficient solution for cylindrical shell based on short and long (enhanced Vlasov's) solutions on example of concentrated radial force // *Proc. of ASME 2018 Pressure Vessels and Piping Conference (July 15–20, 2018, Prague, Czech Republic)*. – Vol. 3A. – 2018. – Paper No: PVP2018-85032, V03AT03A033. – 12 p. – <https://doi.org/10.1115/PVP2018-85032>.
22. Ren D., Fu K.-C. Solutions of complete circular cylindrical shell under concentrated loads // *J. Eng. Mech.* – 2001. – **127**, No. 3. – P. 248–253.  
– [https://doi.org/10.1061/\(ASCE\)0733-9399\(2001\)127:3\(248\)](https://doi.org/10.1061/(ASCE)0733-9399(2001)127:3(248)).
23. Shao W. Y. Thin cylindrical shells subjected to concentrated loads // *Quart. Appl. Math.* – 1946. – **4**, No. 1. – P. 13–26. – [www.jstor.org/stable/43633536](http://www.jstor.org/stable/43633536).
24. Silvestre N. Generalised beam theory to analyse the buckling behaviour of circular cylindrical shells and tubes // *Thin-Walled Struct.* – 2007. – **45**, No. 2. – P. 185–198. – <https://doi.org/10.1016/j.tws.2007.02.001>.

#### ПОРІВНЯННЯ ВЛАСНИХ ФУНКЦІЙ, ВИЗНАЧЕНИХ ДЛЯ ЗАМКНЕНИХ ЦИЛІНДРИЧНИХ ОБОЛОНОК ЗА ДОПОМОГОЮ ІТЕРАЦІЙНОЇ ПРОЦЕДУРИ РОЗЧЕПЛЕННЯ

Запропоновано загальну процедуру визначення власних значень задачі для пружної тонкостінної замкненої циліндричної оболонки, яка полягає у зведенні до диференціального рівняння восьмого порядку. Ідея ґрунтується на розчепленні задачі

на дві простіші: плоску задачу теорії пружності та задачу для пластини, кожна з яких зводиться до біквадратного рівняння. При виборі однієї з цих задач за основу, власні функції іншої задачі знаходимо у вигляді лінійних комбінацій функцій, знайдених з основної задачі. Отримані власні числа порівняно для чотирьох найбільш поширених теорій циліндричних оболонок при навантаженні зосередженою радіальною силою. Результати незначно різняться між собою лише для малих номерів членів розкладу, а також дуже добре узгоджуються з попередніми результатами, отриманими іншими напіваналітичними методами.

**Ключові слова:** циліндрична оболонка, процедура розчеплення, власні числа, зосереджена радіальна сила, головне однорідне рівняння, допоміжний частковий розв'язок.

National Technical University of Ukraine  
“Igor Sikorsky Kyiv Polytechnic Institute”

Received  
08.05.23